ACS Photonics

Article

pubs.acs.org/journal/apchd5

Semiconductor Quantum Dot Lifetime Near an Atomically Smooth Ag Film Exhibits a Narrow Distribution

Thomas Hartsfield,[†] Michael Gegg,[‡] Ping-Hsiang Su,[†] Matthew R. Buck,[§] Jennifer A. Hollingsworth,[§] Chih-Kang Shih,[†,∥] Marten Richter,[‡] Han Htoon,*[,§] and Xiaoqin Li*[,†,∥]

[†]Physics Department and Center for Complex Quantum Systems, University of Texas at Austin, Austin Texas 78712, United States

[‡]Institut für Theoretische Physik, Nichtlineare Optik und Quantenelektronik, Technische Universität Berlin, Berlin, Germany

[§]Materials Physics and Applications Division, Center for Integrated Nanotechnologies, Los Alamos National Laboratory, Los Alamos, New Mexico 87545, United States

[∥]Texas Materials Institute, University of Texas at Austin, Austin, Texas 78712, United States

Supporting Information

ABSTRACT: We investigate photoluminescence from individual "giant" CdSe/CdS core/thick-shell quantum dots (gQDs) placed near an epitaxial Ag film with an atomically smooth surface. The key observation is that the lifetimes of the gQDs are drastically reduced and exhibit a remarkably narrow distribution compared to the gQDs deposited on a thermally deposited Ag film. The larger variations in gQDs' lifetimes on the thermally deposited Ag film arise from excitonic coupling to localized surface plasmons associated with nanoscale surface corrugations of different heights. A calculation is performed based on a simple model system of a QD coupled to a metallic nanosphere. The calculation shows that the QD lifetime initially shortens and reaches a saturated value with increasing radius of the metal nanoparticle (MNP). Because the epitaxial film can be treated as a sphere with an infinitely large radius, the calculation confirms and explains the different QD dynamics near the two types of Ag films as observed experimentally. Our studies demonstrate that epitaxial Ag films serve as an ideal material platform for reliable control over the QD lifetime and may lead to improved photodetectors and light emitting devices requiring fast response or modulation.

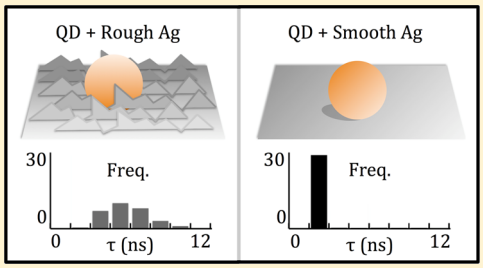

KEYWORDS: *plasmonics, quantum dots, lifetime, epitaxial films, optical spectroscopy*

The lifetime of an emitter is not an intrinsic property of the emitter itself. Instead, it is determined by both the emitter and the photonic density of states of the environment surrounding it. This concept lays the foundation of controlling emitter dynamics through cavity quantum electrodynamics using structures such as photonic crystals. Plasmonic cavities in the form of metallic films and nanostructures have also been explored for this use due to their high photonic density of states and small mode volumes.[1−3] An emitter placed near a plasmonic cavity is affected in multiple ways: an increase in its excitation rate due to the strong near-field, an increase of its radiative decay rate (Purcell effect), and an increase of its nonradiative decay rate due to nonradiative energy transfer.[4−9] The latter two effects combine to strongly reduce the emitter's total excited state lifetime. For example placing a single gold nanoparticle in the immediate proximity of a quantum dot (QD) can decrease the QD lifetime by 2 orders of magnitude or more.[10,11]

A simple model system for investigating modified single emitter dynamics via exciton−plasmon interaction is a semiconductor QD near a planar metal film. A number of studies have explored this geometry and reported reduced lifetimes, modified second order autocorrelation ($g^{(2)}$) photon statistics, and altered blinking behavior.[12−18] In these previous studies, a key challenge to quantitatively predict the modified photoluminescence (PL) properties due to exciton−plasmon interaction lies in the large variations of each QD's local environment due to nanoscale roughness on the metal surface. This variation raises concerns about repeatability and reliability in the performance of devices incorporating QDs and metallic films.

Recent progress in growing high quality single crystalline metal films using molecular beam epitaxy has made it possible to produce Ag films with an atomically smooth surface.[19,20] In this paper, we re-examine the modification of the QD PL lifetimes due to exciton−plasmon interaction by studying individual CdSe/CdS core/thick-shell "giant" QDs (gQDs) placed near such a film. In a way, gQDs act as nanometer-scale sensors that interrogate the local photonic density of states. We found that the lifetime of gQDs near an atomically smooth Ag film displays both a greater reduction in lifetime and a significantly narrower distribution of lifetimes in comparison to dots placed near metal films prepared with conventional thermal evaporation methods. We performed a calculation that reproduced qualitatively the lifetime distribution near the two

Received: March 2, 2016
Published: May 11, 2016

DOI: 10.1021/acsphotonics.6b00151
ACS Photonics 2016, 3, 1085−1089

types of Ag films. Our work demonstrates reliable control of emitter properties using the Ag films with atomically smooth surfaces and the great promise of such films in nanophotonic applications.

We first describe the two types of Ag films used in our experiments: one grown with molecular beam epitaxy on a Si substrate and another prepared using a standard thermal evaporation process. The epitaxially grown Ag film was capped first with ~1.5 nm of MgO and then with 2 nm of Al_2O_3. These oxide layers serve to prevent the Ag film from oxidation and degradation in ambient environment and increase the separation between the gQDs and Ag film as a result. The thermally grown Ag was capped with 3 nm of Al_2O_3 using atomic layer deposition. Atomic force microscopy (AFM) images were taken to characterize the surface topology of the capped Ag films, as shown in Figure 1. The thermally deposited

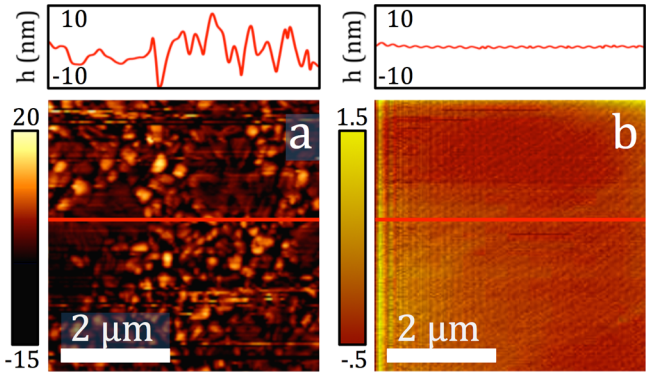

Figure 1. AFM scans of Ag films: (a) AFM scan of the rough Ag film used in this work; the color bar spans 35 nm. A line cut along the red line is plotted above the scan. (b) AFM scan of the atomically smooth Ag film; the color bar spans 2 nm.

Ag film has surface corrugation with large height variations, visible from a line cut through the AFM image. The root-mean-square (RMS) variation of the island heights is 3.57 nm shown in Figure 1a. In contrast, the AFM image taken from the epitaxial Ag proves the atomic smoothness of the surface. The height variation across the smooth Ag film is less than the 0.4 nm resolution limit imposed by noise inherent to the AFM scan shown in Figure 1b; the thickness of a single Ag atomic layer is approximately 0.25 nm. Recent experiments characterizing fundamental properties of single crystalline Ag have also shown that these high quality films exhibit lower loss and support surface plasmon polaritons with long propagation distance, exceeding what has been considered possible based on the widely cited permittivity constants.[21,22] Because of their different surface topology, we anticipate that gQDs placed on these Ag films would interact with different surface plasmon modes and, therefore, exhibit different PL properties.

We use specially synthesized CdSe/CdS gQDs (Methods) with a core diameter of approximately 3.5 nm and a shell thickness of ~8 nm, leading to a diameter of 19.5 nm for the whole gQD. gQDs were chosen as they exhibit the unique properties of being nonblinking and highly resistant to photobleaching.[23−26] In addition, the increased shell thickness compared to standard core/shell QDs reduces nonradiative energy transfer to plasmonic nanostructures. gQDs were prepared on three different substrates: a glass substrate as a reference and the two types of Ag films. The QDs were drop-cast onto these substrates at densities of ~0.1 gQD/μm^2. The experimental setup used for measuring PL lifetime from individual gQDs is described in detail in Methods.

We investigate PL from many individual gQDs on each of the three different substrates and present the results in Figure 2.

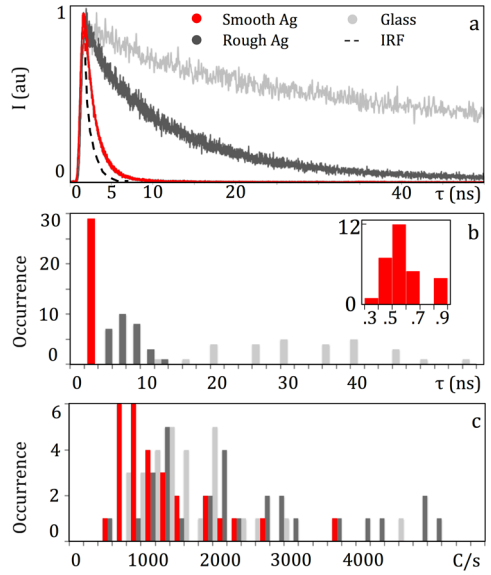

Figure 2. Statistical comparison of PL properties of gQDs on glass, rough Ag and smooth Ag films: (a) A typical PL lifetime measurement of a single gQD on each substrate. (b) Statistical distribution of gQD PL lifetimes on each substrate; inset shows a detailed distribution of gQD lifetimes on smooth Ag in ns. (c) Statistical distributions of average PL intensity on each substrate.

The second order correlation $g^{(2)}$ measurements are performed to confirm that individual gQDs are measured (see Supporting Information for details). The representative exciton lifetime decays for a single gQD on each of these substrates are shown in Figure 2a. It is apparent that the gQD lifetime on Ag films is significantly reduced from the values observed on glass substrates. Because there are usually known variations in lifetime between gQDs, we investigate ~30 different gQDs on each type of substrate. The statistical results of the lifetime measurements are shown in Figure 2b. The mean values and standard deviations of these measurements provide a better characterization than ensemble measurements of many gQDs, which provide only an averaged behavior but no information on the variations between gQDs. The statistical analysis of these measurements yields the average gQD lifetime and the standard deviation as the following: 33 ± 11 (glass), 6 ± 2 (rough Ag film), and 0.6 ± 0.2 ns (epitaxial Ag film). The absolute value of the standard deviation is expected to be smaller for a smaller mean value for the case of the atomically smooth film. However, the same ratio between the mean lifetime and the standard deviation for these two types of films is a coincidence because the distributions have different origins. The lifetime distribution quoted for the epitaxial film is close to the temporal resolution limit of our instruments after signal deconvolution. Nevertheless, we expect some remaining variations in lifetimes due to variations in QD properties and the different nanocrystal crystalline axis orientations leading to different orientation of dipole moments with respect to the metal surface. In contrast, the broader lifetime distribution near the thermally evaporated film mainly arises from variations in the local plasmonic modes and their coupling to the QDs.

DOI: 10.1021/acsphotonics.6b00151
ACS Photonics 2016, 3, 1085−1089

PL intensity on three different substrates did not exhibit obvious differences. The gQD PL intensity near a Ag film is determined by the increased excitation rate by the near field of the film, modified decay rates, and excitation conditions. While an Ag film usually enhances the excitation rate of QDs due to the strong near field, it also increases both the radiative and nonradiative decay rate. Furthermore, our experiments were performed using a pulsed excitation source, where the laser repetition rate limits the photon cycling rate. These effects combined to produce only small differences in the total gQD PL intensity on the two types of Ag films.

To provide a more quantitative explanation for the difference between gQD lifetimes on the two types of Ag films, we perform a calculation to model the coupling of a point dipole to plasmonic modes supported by these films. The fluctuations of the rough surface of the thermally grown Ag film are treated as spherical metal nanoparticles (MNPs) with varying diameters, while the epitaxial film is treated as a MNP with an infinitely large radius. We lack precise information on the shape and size of the surface nanostructures. This model is intended to only capture the QD dynamics qualitatively. The interaction strength between the MNPs and a QD decreases rapidly with increasing distance. Therefore, to a good approximation, the interaction of the QD with the rough Ag surface can be described by a single, spherical MNP surrounded by a capping layer as illustrated in Figure 3a. In this picture, the MNP represents the nearest convexity on the surface.

We calculate the decay kinetics of the QD coupling to a MNP explicitly taking into account multipolar surface plasmon modes. Furthermore, we assume a normal distribution of diameters to calculate the distribution of lifetimes. The calculation of the QD lifetime follows the theory previously developed by Welsch et al.[27,28] and Hughes et al.[29,30] For small MNP radii, the QD lifetime decreases monotonically with increasing MNP radius as shown in Figure 3b. The distribution of QDs' lifetime due to the MNP's diameter distribution is shown in Figure 3c, yielding the mean value in lifetime of 9.9 ns. Consistent with the experimental observation, the calculated lifetime exhibits an asymmetrical distribution. The interval that contains ~31.7% probability (1σ interval) to each side of the mean corresponds to a calculated lifetime of $9.9 - 2.8 + 3.4$ ns, respectively.

In contrast to the wide distribution of the gQD lifetime near the rough thermally evaporated film, this distribution near an epitaxial film is significantly narrower. Our calculation suggests that the exciton lifetime as a function of the MNP radius reaches a minimum near ~35 nm. For MNP with larger radii, the gQD lifetime fluctuates but remains close to ~1 ns. Thus, a narrow distribution of gQD lifetime near the epitaxial film is consistent with our calculation in which the epitaxial film is treated as an infinitely large MNP. These results are also consistent with an alternative model that we have analyzed (results not included explicitly here). In this alternative model, we studied how the QD lifetime changes near a perfectly flat metal slab with increasing thickness. Our calculation suggests that QD lifetime near a metal slab no longer changes once the slab thickness exceeds tens of nanometers.

Qualitatively, the QD lifetime initially decreases with increasing MNP radius because the MNP dipole moment and thus the coupling strength with the QD increases. Higher multipole contributions become more important with increasing radius, essentially leading to a more efficient decay and a shorter QD lifetime. The near field confinement and high density of photonic states associated with the MNP are mainly responsible for QD lifetime reduction. This confinement effect becomes less pronounced when the MNP radius further increases and saturates. The theory seems to generally overestimate the lifetimes, which is likely to be a systematic error. For example, the spacing between the QDs and the films is not accurately known due to uncertainties in the thickness of the oxide layers. To achieve a further reduction of QD lifetime, one may choose QDs with a thinner shell or a better spectral alignment between the exciton and plasmon resonance energy.

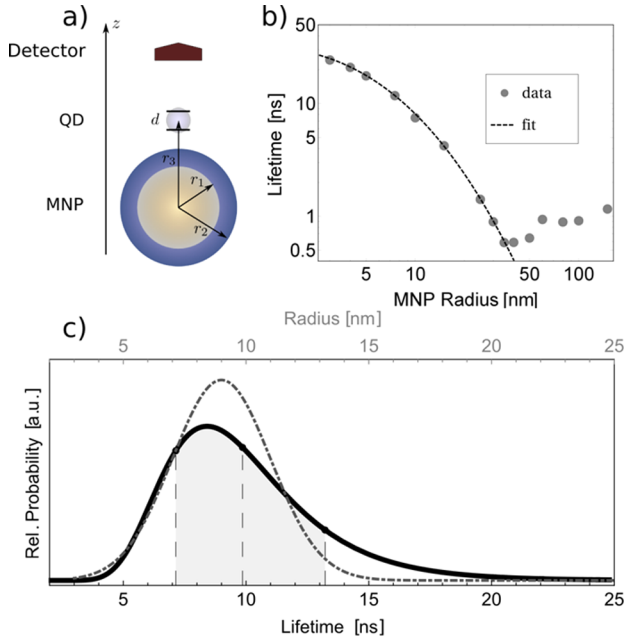

Figure 3. Calculation of QD lifetimes near a metallic sphere. (a) Rough Ag surface is treated as MNPs of varying diameter surrounded by a capping layer of Al_2O_3. The QD is treated as a point dipole located at the center of the giant colloidal QD. The whole setup is aligned along the z axis. (b) Lifetime as a function of radius: The dependence of the lifetime on the radius is monotonic for radius < 35 nm. At radius = 35 nm, the curve has a minimum at 0.6 ns. For higher radii the lifetime fluctuates around 1 ns which can be ascribed to the lifetime of a dot on a slab. We fit the small radius region in order to calculate the lifetime distribution. (c) Lifetime distribution: Based on the AFM scans we assume a normal distribution of mean 9 nm and variance 3 nm for the MNP radii (gray dashed line). Using this distribution and the fit function from (b), we can calculate the statistical distribution of QD lifetimes on the rough Ag surface (black line). The mean of this distribution is 9.9 ns, and the 1 σ interval is the gray shaded area.

In summary, we have investigated how gQD dynamics are modified near Ag films. We demonstrate that the morphology of the films plays a key role in lifetime reduction. By using epitaxial Ag films with atomically smooth surfaces, one can observe drastically reduced gQD lifetimes. More importantly, the reduced lifetimes exhibit a very narrow distribution, demonstrating reliability and reproducibility in lifetime control, which is often missing in previous studies of QDs coupled to a thermally evaporated Ag film. Our calculation shows that the QD lifetime initially drops with increasing MNP radius but saturates beyond a certain MNP size. This saturation effect together with the atomically smooth surface of the epitaxial Ag film is responsible for the narrow distribution of gQD lifetimes. Hybrid photonic devices incorporating both semiconductor emitters and metallic structures will benefit from better decay

DOI: 10.1021/acsphotonics.6b00151
ACS Photonics 2016, 3, 1085−1089

dynamics control as demonstrated in our studies. More dramatic QD lifetime reduction has been achieved via coupling to plasmonic antennas.[31] However, the simple geometry used in our studies does not require the precise placement of the QDs at the gap of an antenna and removes the influence from variations in plasmonic nanostructures (e.g., size and shape), enabling reliable lifetime control as demonstrated. We anticipate that progress in synthesis and growth of smooth metallic films will lead to other exciting progress in the fields of plasmonics and hybrid nanophotonics.

METHODS

Preparation of Epitaxial and Thermally Evaporated Ag Films. The epitaxial Ag film was prepared using molecular beam epitaxy following a refined two-step growth process. First, a small amount of Ag (~20 monolayers) was evaporated at a slow deposition rate of ~1 Å min onto a liquid nitrogen cooled Si(111) substrate (~90 K). Then, the temperature was slowly raised to room temperature to naturally anneal the sample. The final film thickness was determined by the number of iterations of this two-step process. A commercial Knudsen cell was used as the Ag evaporator to ensure a precise and stable deposition rate. The thickness of the films was measured by a quartz crystal monitor during growth. The thermally evaporated film was prepared in a commercial deposition system. A vacuum chamber was evacuated to $\sim 5 \times 10^{-5}$ Torr and growth of Ag began at a deposition rate of ~0.5 nm/s. A total of 50 nm of Ag was deposited. A thin oxide layer, ~3 nm of Al_2O_3, was then grown onto the bare Ag surface using atomic layer deposition.

gQD Preparation. CdSe/CdS gQDs were synthesized according to a modified successive ionic layer adsorption and reaction (SILAR) method for monolayer-by-monolayer shell addition.[25] In this way, CdS shell (monolayer thickness: 0.3375 nm) was added to CdSe QD cores (3.5 nm diameter). Ultradilute solutions were deposited onto the three substrates to obtain a dot density of ~0.1 gQD/μm^2. Importantly, dilution of the stock gQD solution was conducted immediately prior to sample preparation to avoid gQD aggregation that occurs at very low solution concentrations. Absorption spectroscopy and TEM are used to determine the gQD core size, and TEM is used to assess the final gQD size. Ensemble photoluminescence measurements showed a PL peak at ~640 nm.

PL Measurements. The excitation source was a picosecond pulsed diode laser (PicoQuant) with a central wavelength of 405 nm and a variable repetition rate; we used repetition rates between 1 and 5 MHz. The laser is focused through a microscope objective (100× Olympus, N.A. = 0.80) to a spot of ~0.5 μm diameter. The PL was collected through the same objective lens. Excitation power was held constant, and typical time-averaged powers ranged from 1.5 to 7 nW with varying repetition rates. The PL was collected through the same objective lens. The collected signal was sent through a 50/50 beam splitter for $g^{(2)}$ measurement. The single photons were detected by a pair of avalanche photodiodes (APDs, Perkin & Elmer) and the APD outputs were sent to the correlated single photon counting electronics (PicoQuant HydraHarp 400). Time gated $g^{(2)}$ analyses were performed following a procedure as previously described.[32,33]

Theory. We use the theoretical framework developed by Welsch et al.[27,28] and Hughes et al.[29,30] to describe the modified QDs lifetime near a metal nanoparticle. Within this framework, the electromagnetic modes supported by arbitrary spatial structures including dissipating dielectrics are rigorously quantized, while the geometry of the system is included via the classical dyadic Green's function. We assume a spherical MNP, surrounded by a spherical, dielectric shell of Al_2O_3 ($n \sim 1.8$)[34] in vacuum ($n = 1$), that is, a spherically three-layered system[35] illustrated in Figure 3a. Complex dielectric response of the MNP is modeled using data obtained from the atomically smooth Ag film[21] and fitted with a fourth order polynomial. The QD is assumed to be a point dipole located at the center of the giant colloidal CdSe/CdS QD (with a diameter of ~19.5 nm). The emission spectra at detector position are given by

$$S(r,\omega) = \left| \frac{\omega^2}{\epsilon_0 c^2} \frac{\boldsymbol{d}\cdot\boldsymbol{G}_s(\boldsymbol{r},\boldsymbol{r_d},\omega)(\omega-\omega_d)}{\omega_d^2-\omega^2-2\omega_d\omega^2\boldsymbol{d}\cdot\boldsymbol{G}_s(\boldsymbol{r},\boldsymbol{r_d},\omega)(\omega-\omega_d)\cdot\boldsymbol{d}/(\hbar\epsilon_0 c^2)} \right|^2$$

Here $\boldsymbol{G}_s(\boldsymbol{r},\boldsymbol{r_d},\omega)$ is the classical Green's function of the spherically layered MNP−coating−vacuum system, ω_d is the transition frequency of the QD and $\boldsymbol{d}$ is the associated transition dipole moment. In Figure 3a, the geometry of the system is illustrated. The outline of the full calculation can be found in the Supporting Information; for further details, we refer to the literature, that is, refs27−30. The spectral shape is a Fano resonance instead of a Lorentzian, as shown in Figure S2 in the online Supporting Information. Lifetimes are determined via fitting using an exponential function in the time domain. The lifetime distribution is calculated by fitting the dependence of the lifetime on the MNP radius as shown in Figure 3b.

ASSOCIATED CONTENT

Supporting Information

The Supporting Information is available free of charge on the ACS Publications website at DOI: 10.1021/acsphotonics.6b00151.

$g^{(2)}$ measurements of PL signal from individual QDs near epi-Ag film and a more detailed description of the theory treating QD-MNP coupling (PDF).

AUTHOR INFORMATION

Corresponding Authors

*E-mail: htoon@lanl.gov.

*E-mail: elaineli@physics.utexas.edu.

Notes

The authors declare no competing financial interest.

ACKNOWLEDGMENTS

The work at UT-Austin is supported by NSF DMR-1306878 and EFMA-1542747 and Welch Foundation F-1662 and F-1672. M.G. and M.R. acknowledge support by the Deutsche Forschungsgemeinschaft through Sfb 951 and thank Andreas Knorr for fruitful discussions. X.L. also gratefully acknowledges the support from a Humboldt fellowship, which facilitated the collaboration between UT-Austin and TU-Berlin and from NT 3.0 program, Ministry of Education, Taiwan. This work was conducted in part at the Center for Integrated Nanotechnologies (CINT), a U.S. Department of Energy (DOE), Office of Basic Energy Sciences (OBES), Nanoscale Science Research Center and User Facility under User Project C2013B0047. H.H. and J.A.H. acknowledge the support of a Division of Materials Science and Engineering, OBES, Office of Science, DOE Grant (2009LANL1096) for the synthesis and photophysical description of gQDs. M.R.B. was supported by Los Alamos National Laboratory Directed Research and Development Funds.

DOI: 10.1021/acsphotonics.6b00151
ACS Photonics 2016, 3, 1085−1089

REFERENCES

(1) Russell, K. J.; Liu, T.-L.; Cui, S.; Hu, E. L. Large spontaneous emission enhancement in plasmonic nanocavities. *Nat. Photonics* **2012**, *6*, 459−462.

(2) Vesseur, E. J. R.; de Abajo, F. J. G.; Polman, A. Broadband Purcell enhancement in plasmonic ring cavities. *Phys. Rev. B: Condens. Matter Mater. Phys.* **2010**, *82*, 165419.

(3) Tame, M. S.; McEnery, K.; Özdemir, Ş.; Lee, J.; Maier, S.; Kim, M. Quantum plasmonics. *Nat. Phys.* **2013**, *9*, 329−340.

(4) Anger, P.; Bharadwaj, P.; Novotny, L. Enhancement and quenching of single-molecule fluorescence. *Phys. Rev. Lett.* **2006**, *96*, 113002−113002.

(5) Bayer, M.; Reinecke, T.; Weidner, F.; Larionov, A.; McDonald, A.; Forchel, A. Inhibition and enhancement of the spontaneous emission of quantum dots in structured microresonators. *Phys. Rev. Lett.* **2001**, *86*, 3168.

(6) Kühn, S.; Håkanson, U.; Rogobete, L.; Sandoghdar, V. Enhancement of single-molecule fluorescence using a gold nanoparticle as an optical nanoantenna. *Phys. Rev. Lett.* **2006**, *97*, 017402.

(7) Ringler, M.; Schwemer, A.; Wunderlich, M.; Nichtl, A.; Kürzinger, K.; Klar, T.; Feldmann, J. Shaping emission spectra of fluorescent molecules with single plasmonic nanoresonators. *Phys. Rev. Lett.* **2008**, *100*, 203002.

(8) Shimizu, K.; Woo, W.; Fisher, B.; Eisler, H.; Bawendi, M. Surface-enhanced emission from single semiconductor nanocrystals. *Phys. Rev. Lett.* **2002**, *89*, 117401.

(9) Leitner, A.; Lippitsch, M.; Draxler, S.; Riegler, M.; Aussenegg, F. Fluorescence properties of dyes adsorbed to silver islands, investigated by picosecond techniques. *Appl. Phys. B: Photophys. Laser Chem.* **1985**, *36*, 105−109.

(10) Ratchford, D.; Shafiei, F.; Kim, S.; Gray, S. K.; Li, X. Q.Manipulating Coupling between a Single Semiconductor Quantum Dot and Single Gold Nanoparticle. *Nano Lett.* **2011**, *11*, 1049−1054.

(11) Hoang, T. B.; Akselrod, G. M.; Mikkelsen, M. H. Ultrafast room-temperature single photon emission from quantum dots coupled to plasmonic nanocavities. *Nano Lett.* **2016**, *16*, 270−275.

(12) Ito, Y.; Matsuda, K.; Kanemitsu, Y. Mechanism of photoluminescence enhancement in single semiconductor nanocrystals on metal surfaces. *Phys. Rev. B: Condens. Matter Mater. Phys.* **2007**, *75*, 033309.

(13) LeBlanc, S. J.; McClanahan, M. R.; Jones, M.; Moyer, P. Enhancement of multiphoton emission from single CdSe quantum dots coupled to gold films. *Nano Lett.* **2013**, *13*, 1662−1669.

(14) Park, Y.-S.; Ghosh, Y.; Chen, Y.; Piryatinski, A.; Xu, P.; Mack, N. H.; Wang, H.-L.; Klimov, V. I.; Hollingsworth, J. A.; Htoon, H. Super-Poissonian Statistics of Photon Emission from Single CdSe-CdS Core-Shell Nanocrystals Coupled to Metal Nanostructures. *Phys. Rev. Lett.* **2013**, *110*, 117401.

(15) Chi, Y.; Chen, G.; Jelezko, F.; Wu, E.; Zeng, H. Enhanced photoluminescence of single-photon emitters in nanodiamonds on a gold film. *IEEE Photonics Technol. Lett.* **2011**, *23*, 374−376.

(16) Hellen, E. H.; Axelrod, D. Fluorescence emission at dielectric and metal-film interfaces. *J. Opt. Soc. Am. B* **1987**, *4*, 337−350.

(17) Amos, R. M.; Barnes, W. L. Modification of the spontaneous emission rate of Eu^{3+} ions close to a thin metal mirror. *Phys. Rev. B: Condens. Matter Mater. Phys.* **1997**, *55*, 7249−7254.

(18) Wu, X.; Sun, Y.; Pelton, M. Recombination rates for single colloidal quantum dots near a smooth metal film. *Phys. Chem. Chem. Phys.* **2009**, *11*, 5867−5870.

(19) Smith, A. R.; Chao, K.-J.; Niu, Q.; Shih, C.-K. Formation of atomically flat silver films on GaAs with a″ silver mean″ quasi periodicity. *Science* **1996**, *273*, 226−228.

(20) Lu, Y.-J.; Kim, J.; Chen, H.-Y.; Wu, C.; Dabidian, N.; Sanders, C. E.; Wang, C.-Y.; Lu, M.-Y.; Li, B.-H.; Qiu, X. Plasmonic nanolaser using epitaxially grown silver film. *Science* **2012**, *337*, 450−453.

(21) Wu, Y. W.; Zhang, C. D.; Estakhri, N. M.; Zhao, Y.; Kim, J.; Zhang, M.; Liu, X. X.; Pribil, G. K.; Alu, A.; Shih, C. K.; Li, X. Q.Intrinsic Optical Properties and Enhanced Plasmonic Response of Epitaxial Silver. *Adv. Mater.* **2014**, *26*, 6106.

(22) Wang, C.-Y.; Chen, H.-Y.; Sun, L.; Chen, W.-L.; Chang, Y.-M.; Ahn, H.; Li, X.; Gwo, S. Giant colloidal silver crystals for low-loss linear and nonlinear plasmonics. *Nat. Commun.* **2015**, *6*, 7734.

(23) Chen, Y.; Vela, J.; Htoon, H.; Casson, J. L.; Werder, D. J.; Bussian, D. A.; Klimov, V. I.; Hollingsworth, J. A. Giant" multishell CdSe nanocrystal quantum dots with suppressed blinking. *J. Am. Chem. Soc.* **2008**, *130*, 5026−5027.

(24) Vela, J.; Htoon, H.; Chen, Y.; Park, Y. S.; Ghosh, Y.; Goodwin, P. M.; Werner, J. H.; Wells, N. P.; Casson, J. L.; Hollingsworth, J. A. Effect of shell thickness and composition on blinking suppression and the blinking mechanism in 'giant'CdSe/CdS nanocrystal quantum dots. *J. Biophotonics* **2010**, *3*, 706−717.

(25) Ghosh, Y.; Mangum, B. D.; Casson, J. L.; Williams, D. J.; Htoon, H.; Hollingsworth, J. A. New insights into the complexities of shell growth and the strong influence of particle volume in nonblinking "giant" core/shell nanocrystal quantum dots. *J. Am. Chem. Soc.* **2012**, *134*, 9634−9643.

(26) Mangum, B. D.; Sampat, S.; Ghosh, Y.; Hollingsworth, J. A.; Htoon, H.; Malko, A. V. Influence of the core size on biexciton quantum yield of giant CdSe/CdS nanocrystals. *Nanoscale* **2014**, *6*, 3712−3720.

(27) Dung, H. T.; Buhmann, S. Y.; Knöll, L.; Welsch, D.-G.; Scheel, S.; Kästel, J. Electromagnetic-field quantization and spontaneous decay in left-handed media. *Phys. Rev. A: At., Mol., Opt. Phys.* **2003**, *68*, 043816.

(28) Dung, H. T.; Knöll, L.; Welsch, D.-G. Spontaneous decay in the presence of dispersing and absorbing bodies: General theory and application to a spherical cavity. *Phys. Rev. A: At., Mol., Opt. Phys.* **2000**, *62*, 053804.

(29) Van Vlack, C.; Kristensen, P. T.; Hughes, S. Spontaneous emission spectra and quantum light-matter interactions from a strongly coupled quantum dot metal-nanoparticle system. *Phys. Rev. B: Condens. Matter Mater. Phys.* **2012**, *85*, 075303.

(30) Yao, P.; Van Vlack, C.; Reza, A.; Patterson, M.; Dignam, M.; Hughes, S. Ultrahigh Purcell factors and Lamb shifts in slow-light metamaterial waveguides. *Phys. Rev. B: Condens. Matter Mater. Phys.* **2009**, *80*, 195106.

(31) Hoang, T. B.; Akselrod, G. M.; Argyropoulos, C.; Huang, J.; Smith, D. R.; Mikkelsen, M. H. Ultrafast spontaneous emission source using plasmonic nanoantennas. *Nat. Commun.* **2015**, *6*, 7788.

(32) Mangum, B. D.; Ghosh, Y.; Hollingsworth, J. A.; Htoon, H. Disentangling the effects of clustering and multi-exciton emission in second-order photon correlation experiments. *Opt. Express* **2013**, *21*, 7419−7426.

(33) Wang, F.; Karan, N. S.; Nguyen, H. M.; Mangum, B. D.; Ghosh, Y.; Sheehan, C. J.; Hollingsworth, J. A.; Htoon, H. Quantum Optical Signature of Plasmonically Coupled Nanocrystal Quantum Dots. *Small* **2015**, *11*, 5028−5034.

(34) Malitson, I.; Dodge, M. In *Refractive-index and birefringence of synthetic sapphire*. *J. Opt. Soc. Am.* **1972**, *62*, 1405−1405.

(35) Li, L.-W.; Kooi, P.-S.; Leong, M.-S.; Yee, T.-S. Electromagnetic dyadic Green's function in spherically multilayered media. *IEEE Trans. Microwave Theory Tech.* **1994**, *42*, 2302−2310.

DOI: 10.1021/acsphotonics.6b00151
ACS Photonics 2016, 3, 1085−1089